A&A manuscript no.
(will be inserted by hand later)

Your thesaurus codes are:
08 (08.01.1; 08.16.4; 08.05.3; 08.09.3;)

ASTRONOMY AND ASTROPHYSICS

August 6, 1999

On the formation of hydrogen-deficient post-AGB stars

F. Herwig[1], T. Blöcker[2], N. Langer[1] and T. Driebe[2]

[1] Universität Potsdam, Institut für Physik, Astrophysik, Am Neuen Palais 10, D-14469 Potsdam
email: fherwig@astro.physik.uni-potsdam.de, ntl@astro.physik.uni-potsdam.de
[2] Max-Planck-Institut für Radioastronomie, Auf dem Hügel 69, D-53121 Bonn
email: bloecker@speckle.mpifr-bonn.mpg.de, driebe@speckle.mpifr-bonn.mpg.de

Received ; accepted

Abstract. We present an evolutionary sequence of a low mass star from the Asymtotic Giant Branch (AGB) through its post-AGB stage, during which its surface chemical composition changes from hydrogen-rich to strongly hydrogen-deficient as consequence of a very late thermal pulse, following the so-called *born-again scenario*. The internal structure and abundance changes during this pulse are computed with a numerical method which allows the physically consistent calculation of stellar layers where thermonuclear and mixing time scale are comparable — a situation which occurs when the helium flash driven convection zone extends to the hydrogen-rich surface layers during the pulse peak. The final surface mass fractions are [He/C/O]=[0.38/0.36/0.22], where the high oxygen abundance is due to diffusive overshoot employed during the AGB evolution. These models are the first to achieve general agreement with the surface abundance pattern observed in hydrogen-deficient post-AGB stars — e.g. the PG 1159 stars or the WR-type central stars of planetary nebulae —, confirming the born-again scenario with a physically consistent calculation and supporting the occurrence of convective overshooting in thermally pulsing AGB stars.

Key words: Stars: abundances – Stars: AGB and post-AGB – Stars: evolution – Stars: interiors

1. Introduction

Stars on the so called Asymptotic Giant Branch (AGB) have strong stellar winds, which gradually reduce the mass of the hydrogen-rich stellar envelope. When this envelope mass falls below a critical value, the stars leave the AGB to become post-AGB stars, central stars of planetary nebulae (CSPNe), and finally white dwarfs. Post-AGB stars show a variety of surface abundances (Méndez, 1991). About 80% of all CSPNe show a solar-like composition while the remaining ones are hydrogen-deficient. Among the latter are Wolf-Rayet type CSPNe ([WR]-CSPNe) and the extremly hot PG 1159 stars with typical surface abundances of [He/C/O]=[0.33/0.50/0.17] (Dreizler and Heber (1998); see also Koesterke and Hamann (1997) and references in both papers). Hydrogen-deficiency is also found in white dwarfs of spectral type DO (Dreizler and Werner, 1996).

The origin of the hydrogen-deficiency in post-AGB stars is a longstanding problem. Most post-AGB calculations predict a hydrogen-rich surface composition (Schönberner, 1979; Schönberner, 1983; Wood and Faulkner, 1986; Vassiliadis and Wood, 1994; Blöcker, 1995a; Blöcker and Schönberner, 1997). So far, no post-AGB models reproduced the observed high carbon and oxygen abundance. The most promising scenario for obtaining a hydrogen-deficient surface composition envokes a very late thermal pulse (Fujimoto, 1977; Schönberner, 1979; Iben et al., 1983) — i.e. a pulse which occurs after the star has already left the AGB — during which the pulse driven convection zone can mix hydrogen-free material out to the stellar surface. Within this *born-again scenario*, Iben and McDonald (1995) obtain surface mass fractions of [He/C/O]=[0.76/0.15/0.01], i.e. their model indeed became strongly hydrogen-deficient. Hovever, the large oxygen abundance found in most H-deficient post-AGB stars could not be reproduced be these, nor by any other calculation. These difficulties have posed a strong limitation to the whole scenario.

In this *Letter* we present a post-AGB model sequence starting from an AGB model computed with overshoot (Herwig et al., 1997), and using a numerical method of computing nuclear burning and time-dependent convective mixing simultaneously.

2. Numerical method

The stellar models are based on the stellar evolution code described by Blöcker (1995b). However, the treatment of the chemical evolution was entirely replaced by a numerical scheme which solves the time dependence of the considered nuclear species — i.e., the changes due to thermonuclear reactions and due to mixing — in one single step. This enables us, in contrast to earlier investigations of very late thermal pulses, to reliably predict the chemical abundance profiles and the nuclear energy generation rates in situations where the time scales of nuclear burning and mixing are comparable. The abundance

Send offprint requests to: F. Herwig

change for each isotope at each mesh point due to diffusive mixing and nuclear processing is given by

$$\left(\frac{\mathrm{d}\boldsymbol{X}_j}{\mathrm{d}t}\right) = \frac{\partial}{\partial m}\left[\left(4\pi r^2\rho\right)^2 D\frac{\partial \boldsymbol{X}_j}{\partial m}\right] + \hat{F}_j \cdot \boldsymbol{X}_j, \quad (1)$$

where $\boldsymbol{X}_j$ contains the abundances of all considered isoptopes at the j^{th} mesh point, $\hat{F}_j$ is the nuclear rate matrix, D is the diffusion coefficient describing the efficiency of convective mixing, r is the radius and ρ the density. This leads to a set of non-linear equations with $M \cdot N$ unknowns, where M is the number of grid points and N is the number of isotopes. In the present calculations, M is of the order of 2000, and $N = 15$ as the main thermonuclear reactions for hydrogen burning through the pp chains and the CNO cycle as well as the main helium burning reactions are included. The solution is obtained fully implicit with a Newton-Raphson iteration scheme by making use of the band-diagonal structure of the problem. The scheme converges to sufficient precision within about 3 iterations. A coupled solution of one nuclear reaction at a time and time-dependent mixing, including also the structure equations, has already been applied by Eggleton (1972).

3. The AGB starting model

We start with an AGB model with $M_{\mathrm{ZAMS}} = 2\,\mathrm{M}_\odot$ which has been evolved over 22 thermal pulses, including convective overshoot at all convective boundaries. The treatment and efficiency (f=0.016) of overshoot is the same as in Herwig et al. (1997). In comparison to models without overshoot the intershell region is much stronger enriched in carbon and oxygen (mass fractions [He/C/O]=[0.35/0.43/0.19]), which causes a stronger third dredge-up (Herwig et al., 1999). At the 16^{th} thermal pulse (TP) the hydrogen-free core has a mass of $M_{\mathrm{core}} = 0.573\,\mathrm{M}_\odot$ and dredge-up starts to operate, leading to a carbon star model at the last computed TP. At this stage the model star has a total mass of $M = 1.42\,\mathrm{M}_\odot$ and $M_{\mathrm{core}} = 0.604\,\mathrm{M}_\odot$. We then artificially increase the mass loss ($\dot{M} > 10^{-3}\,\mathrm{M}_\odot/\,\mathrm{yr}$) in order to force the model to leave the AGB at the right phase to develop a very late thermal pulse. This procedure is justified for this exploratory work because it does not affect the nucleosynthesis and mixing during the very late TP.

4. Evolution through the very late thermal pulse

Two cases of the born-again scenario should be distinguished. Depending on the time when the post-AGB thermal pulse occurs, shell hydrogen burning may still be active or may already have ceased.

In the first case, the He-flash driven convection zone cannot extend into the hydrogen-rich envelope due to the entropy barrier generated by the burning shell (Iben, 1976). In the second case, which is realized in our model sequence, hydrogen shell burning is extinct and the star has entered the white dwarf cooling domain (Fig. 1). We designate a TP in this situation as a *very late* TP.

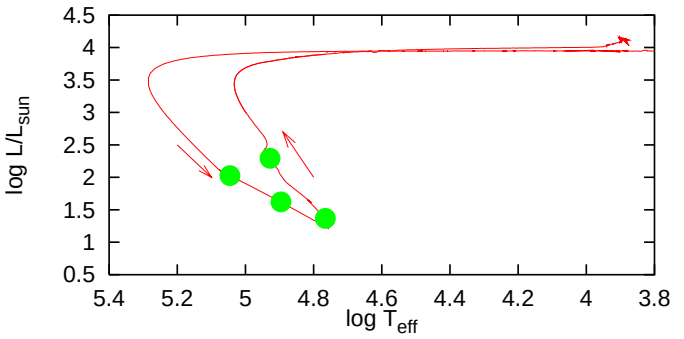

Fig. 1. Track in the HR diagram of our post-AGB model during the evolution through a very late TP. At the first mark along the track, the He-flash has already caused a prominent convectively unstable region. At the second mark, the outwards growing convection zone has reached the envelope and protons start to enter the convective zone (compare Fig. 2 and Fig. 3). At the third mark the hydrogen luminosity has reached its peak (see Fig. 2 and Fig. 4). The surface composition is hydrogen-free beyond the last mark.

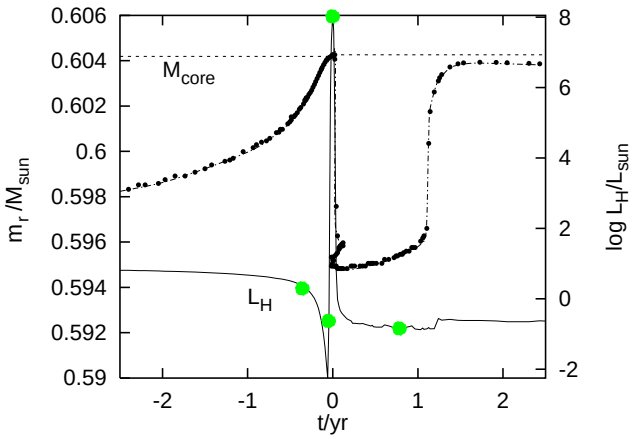

Fig. 2. Evolution of the top boundary of the convection zone (dash-dotted line with filled circle for every second stellar model, left scale) as it extends into the hydrogen-rich envelope, and the nuclear luminosity due to hydrogen burning (solid line, right scale). The four grey dots along the solid line correspond to the marks in Fig. 1. The dashed line shows the mass coordinate of the hydrogen-free core which is for $t > 0\,\mathrm{yr}$ identical with the total stellar mass.

As the helium luminosity increases in the course of the He-flash in our model sequence (first mark in Fig. 1), the corresponding region of convective instability enlarges (Fig. 2). When the upper convective boundary reaches the mass coordinate where the hydrogen abundance increases, convective mixing transports protons downwards into the hot interior (Fig. 3). The protons are at some point captured by ^{12}C via the reaction $^{12}\mathrm{C}(\mathrm{p},\gamma)^{13}\mathrm{N}$. The peak of the resulting luminosity due to hydrogen burning (see also Fig. 2) is located at the mass coordinate where the nuclear time scale equals the mixing time scale ($\simeq$ one hour).

The profile of hydrogen in Fig. 3 and 4 demonstrates that a correct treatment of simultaneous burning and convective mix-

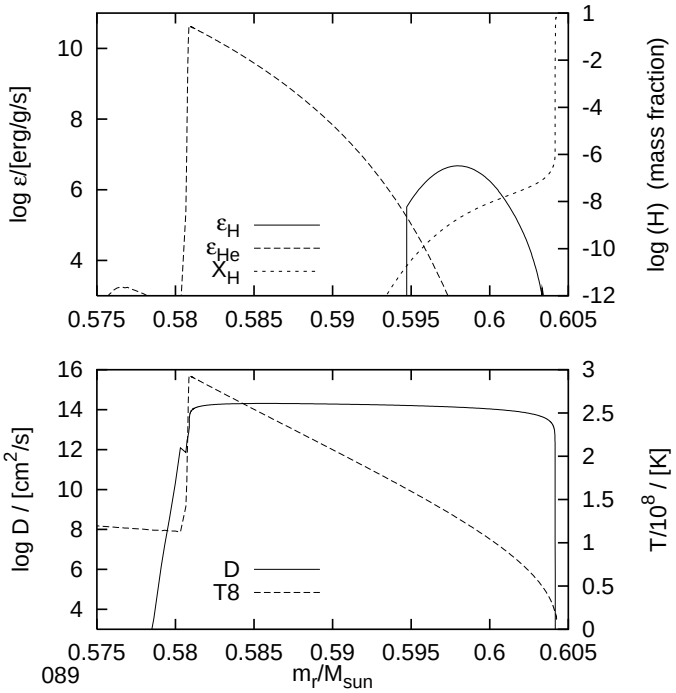

Fig. 3. Internal structure and composition at the onset of hydrogen ingestion into the He-flash convection zone during the very late TP (second mark in Fig. 1). **Top panel:** The nuclear energy generation is dominated by processing of helium at the bottom of the He-flash convection zone. Energy due to proton capture is released in the upper part of the He-flash convection zone (left scale). The hydrogen profile reflects the simultaneous nuclear burning and convective mixing (right scale). The surface composition at this stage is still hydrogen-rich. **Bottom panel:** The diffusion coefficient (left scale) visualizes the convectively unstable region corresponding to the He-flash, which has just reached the lower part of the hydrogen-rich envelope.

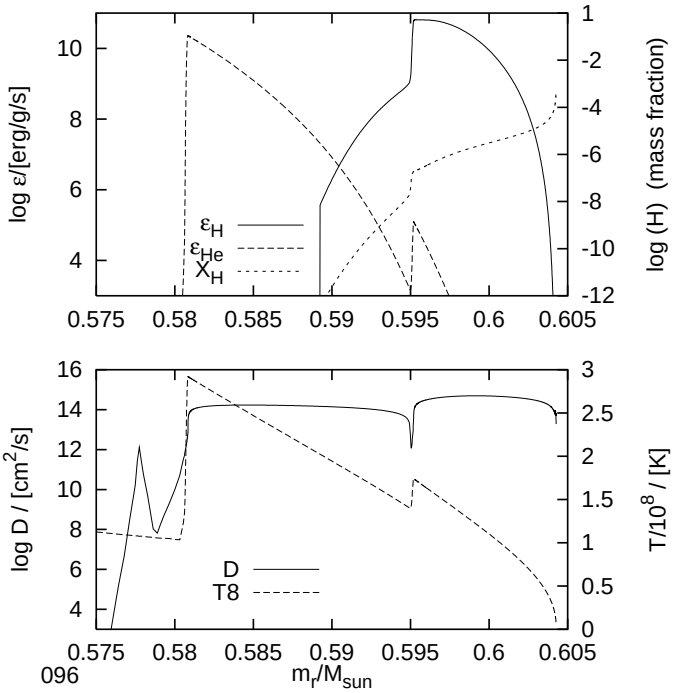

Fig. 4. Internal structure and composition at the time of maximum energy generation due to proton captures (third mark in Fig. 1). **Top panel:** Nuclear energy generation due to hydrogen burning and helium burning (left scale) and hydrogen profile (right scale). **Bottom panel:** The diffusion coefficient (left scale) shows that the convectively unstable region of the thermal pulse is split into two ($m_{\rm r} = 0.595\,{\rm M}_\odot$).

ing is essential for this evolutionary phase. A treatment of convective mixing which does not include the simultaneous computation of the isotopic abundances according to the equations of the nuclear network would fail to predict a correct hydrogen profile. In particular, such a treatment would possibly let the protons travel too deep into the convective region, without considering that they would have been captured already on the way. Then, the energy generation rate due to proton captures may be overestimated and not correctly located.

The energy from proton captures is released in the upper part of the He-flash driven convection zone, which leads to a split (at $m_{\rm r} = 0.595\,{\rm M}_\odot$) of the convective region (Fig. 4). The two convective regions are then connected by the overlapping overshoot extensions, but Fig. 2 shows that the second convective zone is only short lived since the amount of hydrogen available in the envelope is quickly consumed.

Figure 4 shows that the hydrogen burning convection zone extends over $\simeq 10^{-2}\,{\rm M}_\odot$ and reaches from $m_{\rm r} = 0.595\,{\rm M}_\odot$ up to the surface of the stellar model. The surface hydrogen abundance declines rapidly due to mixing and proton captures in the deeper layers. The period of the largest hydrogen burning luminosity (shown in Fig. 4) of $L_{\rm H} \simeq 10^8\,{\rm L}_\odot$ lasts for less than a week, and the whole episode of convective hydrogen burning is a matter of about a month. Overall, $5 \cdot 10^{-5}\,{\rm M}_\odot$ of hydrogen are burnt. At peak hydrogen luminosity the hydrogen mass fraction at the surface is $3.4 \cdot 10^{-4}$ and the total amount of hydrogen still present in the star is $M_{\rm H} = 7.8 \cdot 10^{-6}\,{\rm M}_\odot$. Thus, in this sequence the star is already hydrogen-deficient before it returns to the AGB domain in the HRD.

Figure 5 shows abundance profiles before and after the mixing and burning event due to the very late TP. While the star still shows the typical hydrogen-rich AGB abundance pattern before the convective region has reached into the envelope (top panel, Fig. 5), the mixing during the convective hydrogen burning leads to a hydrogen-free surface with [He/C/O]=[0.38/0.36/0.22] and a mass fraction of 3.5% of neon. The step in the abundances of ^{4}He, ^{12}C and ^{16}O at $0.596\,{\rm M}_\odot$ (lower panel) corresponds to the split of the convective region due to hydrogen burning. While the hydrogen burning leads not to a significant abundance changes for the major isotopes (only $5 \cdot 10^{-5}\,{\rm M}_\odot$ of hydrogen are processed), helium burning continues to process helium at the bottom of the He-flash convective zone. The final surface abundances are very similar to the intershell abundances during the thermal pulse.

After most of the hydrogen is burnt, the corresponding upper convection zone disappears when the local luminosity drops. It takes about one year until the He-flash convec-

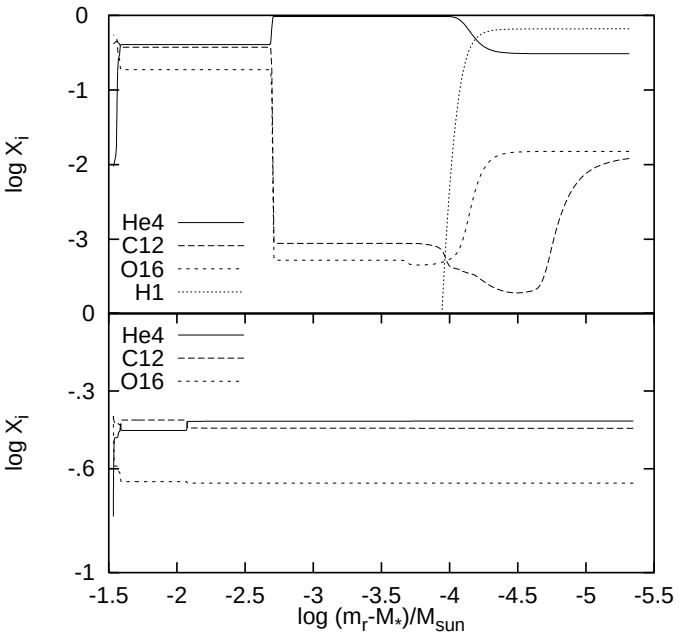

Fig. 5. Chemical profiles (mass fraction vs. mass coordinate) of the upper mass region also covered by Fig. 4. **Top panel:** Profile before the convective region of the He-flash has reached the envelope corresponding to position of first mark in Fig. 1 **Bottom panel:** Profile corresponding to position of last mark in Fig. 1 after all hydrogen has been processed (only trace amounts of $4 \cdot 10^{-11}\,\mathrm{M}_{\odot}$ are left in the whole star), the abundance at the surface differs only slightly from the intershell abundance.

tion zone has recovered to its original extent (Fig. 2). The star then follows the evolution as known from the born-again scenario (for a recent account on this scenario see Blöcker and Schönberner, 1997). Energetically, the return into the AGB domain is almost exclusively driven by the energy release due to helium burning, which exceeds the additional supply of energy from hydrogen burning by orders of magnitude.

5. Conclusions

Using a numerical method to treat nuclear burning and mixing simultaneously in stellar evolution calculations, which allows a reliable and robust modelling of very late thermal pulses, we have shown that the general surface abundance pattern observed in hydrogen-deficient post-AGB stars can be explained within the born-again scenario. Our new post-AGB sequence shows that due to the energy generation and convective mixing during a very late thermal pulse a born-again star forms which displays its previous intershell abundance at the surface.

We have based the calculation on an AGB model sequence computed with overshoot, which shows a high carbon and oxygen intershell abundance. Thus, the fact that the abundance pattern of our post-AGB model after the thermal pulse agrees with the observation of hydrogen-deficient post-AGB stars like PG 1159 and [WC]-CSPNe strongly supports the assumption of extra mixing beyond the convective boundary of the He-convection zone in AGB stars. We conclude that the very late thermal pulses can indeed be identified as one cause for the hydrogen-deficiency in post-AGB stars.

However, we note that not all H-deficient post-AGB stars are completely free of hydrogen (Leuenhagen and Hamann, 1998), as predicted by our model. Other possibilities than the born-again scenario to achieve H-deficiency might also exist (Tylenda, 1996; Waters et al., 1998). Whether post-AGB models which are not entirely hydrogen-free can be obtained within this scenario requires a study of the variation of the late thermal puls with the inter-pulse phase at which the star leaves the AGB (Iben, 1984), and possibly the consideration of other mixing processes, e.g. due to rotational effects (Langer et al., 1999), which has to be left to future investigations.

Acknowledgements. We are grateful to W.-R. Hamann and L. Koesterke for many useful discussions. This work has been supported by the *Deutsche Forschungsgemeinschaft* through grant La 587/16.

References

Blöcker, T., 1995b, A&A 297, 727
Blöcker, T., 1995a, A&A 299, 755
Blöcker, T. and Schönberner, D., 1997, A&A 324, 991
Dreizler, S. and Heber, U., 1998, A&A 334, 618
Dreizler, S. and Werner, K., 1996, in C. S. Jeffery and U. Heber (eds.), Hydrogen-Deficient Stars, Vol. 96, p. 281, ASP Conf. Ser.
Eggleton, P. P., 1972, MNRAS 156, 361
Fujimoto, M. Y., 1977, PASJ 29, 331
Herwig, F., Blöcker, T., and Schönberner, D., 1999, in T. L. Bertre, A. Lebre, and C. Waelkens (eds.), AGB Stars, PASP, in press
Herwig, F., Blöcker, T., Schönberner, D., and El Eid, M. F., 1997, A&A 324, L81
Iben, Jr., I., 1976, ApJ 208, 165
Iben, Jr., I., 1984, ApJ 277, 333
Iben, Jr., I., Kaler, J. B., Truran, J. W., and Renzini, A., 1983, ApJ 264, 605
Iben, Jr., I. and McDonald, J., 1995, in D. Koester and K. Werner (eds.), White Dwarfs, No. 443 in LNP, p. 48, Springer, Heidelberg
Koesterke, L. and Hamann, W. R., 1997, A&A 320, 91
Langer, N., Heger, A., Wellstein, S., and Herwig, F., 1999, A&A 346, L37
Leuenhagen, U. and Hamann, W.-R., 1998, A&A 330, 265
Méndez, R. H., 1991, in G. Michaud and A. Tutukov (eds.), Evolution of Stars:The Photospheric Abundance Connection, p. 375
Schönberner, D., 1979, A&A 79, 108
Schönberner, D., 1983, ApJ 708, 272
Tylenda, R., 1996, in C. S. Jeffery and U. Heber (eds.), Hydrogen-Deficient Stars, Vol. 96, p. 101, ASP Conf. Ser.
Vassiliadis, E. and Wood, P., 1994, ApJS 92, 125
Waters, L. B. F. M., Beintema, D. A., Zijlstra, A. A., and et al., 1998, A&A 331, L61
Wood, P. R. and Faulkner, D. J., 1986, ApJ 307, 659